Density Functional Characterization of the Band Edges, the Band Gap States, and the Preferred Doping Sites of Halogen-Doped TiO_2

Kesong Yang,[†] Ying Dai,*[,†,‡] Baibiao Huang,[‡] and Myung-Hwan Whangbo[§]

School of Physics and State Key Laboratory of Crystal Materials, Shandong University, Jinan 250100, People's Republic of China, and Department of Chemistry, North Carolina State University, Raleigh, North Carolina 27695-8204

Received June 27, 2008. Revised Manuscript Received August 17, 2008

First-principles density functional theory (DFT) electronic structure calculations were carried out for model halogen-doped anatase TiO_2 structures to evaluate the effect of halogen doping on the band edges and the photocatalytic activity of TiO_2. The model structures of X-doped TiO_2 were constructed by using the 48-atom $2 \times 2 \times 1$ supercell of anatase TiO_2 with one O or one Ti atom replaced with X (=F, Cl, Br, I). The unit cell parameters and the atom positions of the resulting X-doped TiO_2 with X at an O site (X@O) and that with X at a Ti site (X@Ti) were optimized by performing first-principles DFT calculations. On the basis of the optimized structures of X-doped TiO_2 with X@O and X@Ti, the defect formation energies and the plots of the density of states were calculated to analyze the band edges, the band gap states, and the preferred doping sites. Our work shows that the doping becomes more difficult in the order F < Cl < Br < I for X-doped TiO_2 with X@O, while the doping becomes less difficult in the order F < Cl < Br < I for X-doped TiO_2 with X@Ti. Under O-rich growth condition, it is energetically more favorable to substitute Br and I for a Ti site than for an O site, while it is energetically more favorable to substitute F and Cl for an O site than for a Ti site. Under Ti-rich condition, it is energetically more favorable to substitute all X (=F, Cl, Br, I) for an O site than for a Ti site. The I atoms in I-doped TiO_2 with I@Ti are present as I^{5+} (s^2) ions, while in X-doped TiO_2 with X@Ti (X = F, Cl, Br) the F, Cl, and Br are present as F^{3+} (s^2p^2), Cl^{4+} (s^2p^1), and Br^{4+} (s^2p^1) ions, respectively. I-doped TiO_2 either with I@Ti or with I@O has a doubly filled band gap state, which significantly reduces the optical band gap with respect to that of undoped TiO_2.

1. Introduction

Titanium dioxide (TiO_2) is a promising photocatalyst due to its high oxidation power, long-term stability, low cost, and nontoxicity. However, the photocatalytic activity of TiO_2 is limited because its large band gap (i.e., 3.2 eV for the anatase phase[1] and 3.0 eV for the rutile phase[2]) makes it inefficient for visible light to generate electron−hole pairs, which are needed for initiating a photocatalytic process. To improve the photocatalytic efficiency of TiO_2 under visible light, numerous attempts have been made to modify the electronic structure of TiO_2 by doping it with various transition metal (Zn, Ni, Co, Mn, etc.)[3−7] and main group (N, S, B, C, P, etc.)[8−12] elements.

In recent years, doping TiO_2 with halogen has received much attention. F-doped TiO_2 samples exhibit an enhanced photocatalytic activity [13,14] and a stronger absorption in the UV/vis region with a slight decrease in the band gap (by about 0.05 eV).[15] A small red-shift of the absorption edge also occurs in F-doped TiO_2 nanotubes.[16] Studies of F-doped TiO_2 prepared by ion implantation [17,18] suggested that F-doping lowers the conduction band (CB) edge of TiO_2, thus reducing the band gap.[18] However, more recent experimental studies suggest that F-doping neither causes any change in the absorption edge of TiO_2 [19−22] nor affects the

* Corresponding author. E-mail: daiy60@sdu.edu.cn.
† School of Physics, Shandong University.
‡ State Key Laboratory of Crystal Materials, Shandong University.
§ North Carolina State University.

(1) Tang, H.; Lévy, F.; Berger, H.; Schmid, P. E. *Phys. Rev. B* **1995**, *52*, 7771.
(2) Arntz, F.; Yacoby, Y. *Phys. Rev. Lett.* **1966**, *17*, 857.
(3) Jing, L.; Xin, B.; Yuan, F.; Xue, L.; Wang, B.; Fu, H. *J. Phys. Chem. B* **2006**, *110*, 17860.
(4) Zhu, S.; Wang, L. M.; Zu, X. T.; Xiang, X. *Appl. Phys. Lett.* **2006**, *88*, 043107.
(5) Mattsson, A.; Leideborg, M.; Larsson, K.; Westin, G.; Osterlund, L. *J. Phys. Chem. B* **2006**, *110*, 1210.
(6) Fu, L. F.; Browning, N. D.; Zhang, S. X.; Ogale, S. B.; Kundaliya, D. C.; Venkatesan, T. *J. Appl. Phys.* **2006**, *100*, 123910.
(7) Gracia, F.; Holgado, J. P.; Caballero, A.; Gonzalez-Elipe, A. R. *J. Phys. Chem. B* **2004**, *108*, 17466.
(8) Asahi, R.; Morikawa, T.; Ohwaki, T.; Aoki, K.; Taga, Y. *Science* **2001**, *293*, 269.
(9) Umebayashi, T.; Yamaki, T.; Itoh, H.; Asai, K. *Appl. Phys. Lett.* **2002**, *81*, 454.
(10) Zhao, W.; Ma, W.; Chen, C.; Zhao, J.; Shuai, Z. *J. Am. Chem. Soc.* **2004**, *126*, 4782.
(11) Khan, S. U. M.; Al-Shahry, M.; Jr, W. B. I. *Science* **2002**, *297*, 2243.
(12) Yu, J. C.; Zheng, Z.; Zhao, J. *Chem. Mater.* **2003**, *15*, 2280.
(13) Hattori, A.; Tada, H. *J.Sol-Gel Sci. Technol.* **2001**, *22*, 47.
(14) Wu, G.; Wang, J.; Thomas, D. F.; Chen, A. *Langmuir* **2008**, *24*, 3503.
(15) Yu, J. C.; Yu, J.; Ho, W.; Jiang, Z.; Zhang, L. *Chem. Mater.* **2002**, *14*, 3808.
(16) Su, Y.; Zhang, X.; Han, S.; Chen, X.; Lei, L. *Electrochem. Commun.* **2007**, *9*, 2292.
(17) Yamaki, T.; Sumita, T.; Yamamoto, S. *J. Mater. Sci. Lett.* **2002**, *21*, 33.
(18) Yamaki, T.; Umebayashi, T.; Sumita, T.; Yamamoto, S.; Maekawa, M.; Kawasuso, A.; Itoh, H. *Nucl. Instrum. Methods Phys. Res., Sect. B* **2003**, *206*, 254.
(19) Li, D.; Haneda, H.; Hishita, S.; Ohashi, N.; Labhsetwar, N. K. *J. Fluorine Chem.* **2005**, *126*, 69.

10.1021/cm801741m CCC: $40.75
Published on Web 09/26/2008

optical absorption of TiO_2.[23−25] The photocatalytic properties of TiO_2 doped with other halogen elements have also been reported. For example, TiO_2 codoped with Cl and Br has a smaller optical band gap.[26] I-doped TiO_2 shows a much better photocatalytic activity than undoped TiO_2 under both visible light and UV−visible light.[27,28] The good photocatalytic properties of I-doped TiO_2 under visible light was considered to originate from a TiO_6 octahedral distortion[29] and surface IO_4 species.[30]

To account for the enhanced photocatalytic properties of halogen-doped TiO_2 under UV/vis light, it is necessary to examine how the CB and valence band (VB) edges, i.e., the CB minimum (CBM) and the VB maximum (VBM), of TiO_2 are modified by the doping and whether the doping introduces band gap states (i.e., states lying in the band gap of undoped TiO_2). In principle, a halogen dopant X (=F, Cl, Br, I) in TiO_2 can occupy an O or a Ti site. The substitution of X for O means that an X^- ion replaces an O^{2-} ion. Since each X atom requires one less electron from the TiO_2 lattice than does each O atom, X-doped TiO_2 with X at an O site should have the Fermi level at the bottom part of the CB. In contrast, the substitution of X for Ti means that X should exist as a cation. In fact, in I-doped anatase and rutile TiO_2, the dopant exists as an I^{5+} (s^2) ion at a Ti^{4+} (d^0) site.[27,28] The latter means that each I atom releases one more electron to the TiO_2 lattice than does each Ti atom, so the Fermi level of I-doped TiO_2 should also lie at the bottom part of the CB. The ionic radius of X^- increases in the order F < Cl < Br < I (i.e., 1.19, 1.81, 1.96, and 2.20 Å, respectively, at a six-coordinate site[31]), while the ionic radius of O^{2-} (1.40 Å at a six-coordinate site[31]) is smaller than that of Cl^-. In terms of ionic size, therefore, the difficulty of doping of X at an O site should increase in the order F < Cl < Br < I. The electronegativity of X decreases in the order F > Cl > Br > I (i.e., 3.91, 3.10, 2.95, and 2.74, respectively), while that of O is 3.41 (here we use the Mulliken electronegativity[32]). Thus, in terms of electronegativity as well, the doping of X at an O site becomes increasingly more difficult in the order F < Cl < Br < I. This might explain why the dopant I prefers a Ti site to an O site in I-doped TiO_2. The ionic radii of Ti^{4+} and I^{5+} at a six-coordinate site are 0.61 and 0.95 Å, respectively. In terms of both ionic size and electronegativity, one cannot exclude the possibility that Br also prefers a Ti site to an O site in Br-doped TiO_2. In principle, replacing an O or a Ti site with an element of different charge can induce a charge imbalance, thus resulting in the formation of a crystallographic point defect, e.g., an oxygen or Ti vacancy. However, the doped TiO_2 is overall electrically neutral, and the charge imbalance associated with a dopant can be compensated by changing the oxidation state of the dopant or another atom of TiO_2. For example, the substitution of F for O (i.e., F^-doping at an O^{2-}site) is considered to convert one $Ti^{4+}$to Ti^{3+},[15,33]and so is the substitution of I for Ti (i.e., I^{5+}doping at a Ti^{4+}site).[34]

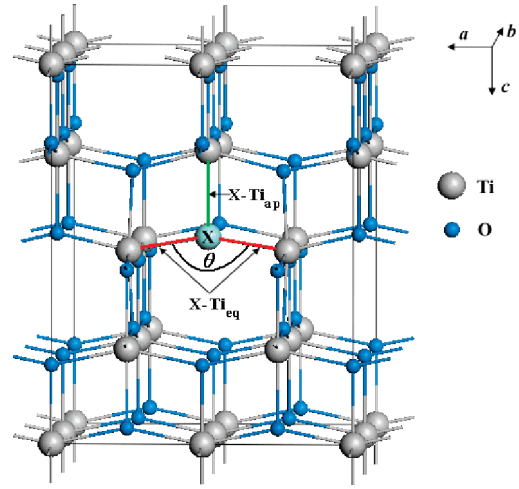

Figure 1. Forty-eight-atom 2 × 2 × 1 supercell model used to simulate X-doped anatase TiO_2 with X@O (X = F, Cl, Br, I). The XTi_3 local geometry is described in terms of the three parameters $X-Ti_{eq}$, $X-Ti_{ap}$, and θ.

Thus, in understanding the electronic structures of X-doped TiO_2 (X = F, Cl, Br, I) and hence the effect of halogen doping on the band edges and the photocatalytic activity of TiO_2, it is important to explore systematically whether X doping in TiO_2 occurs at an O or at a Ti site. In the present work, we examine the band edges, the band gap states, and the preferred doping sites of X-doped TiO_2 (X = F, Cl, Br, I) as well as the site-preference of X in X-doped TiO_2 by performing first-principles density functional theory (DFT) electronic structure calculations for model X-doped TiO_2 structures.

2. Details of Calculations

The structure of X-doped TiO_2 with X at an O site (hereafter referred to as "with X@O") was constructed on the basis of the 48-atom 2 × 2 × 1 supercell by replacing one O atom with one X atom (X = F, Cl, Br, I) (Figure 1). Likewise, the structure of X-doped TiO_2 with X at a Ti site (hereafter referred to as "with X@Ti") was modeled in terms of the 48-atom 2 × 2 × 1 supercell by replacing one Ti atom with one X atom (Figure 2). The first-principles DFT electronic structure calculations were performed with a triclinic space group using the Vienna ab-inito simulation

(20) Li, D.; Haneda, H.; Hishita, S.; Ohashi, N. *Chem. Mater.* **2005**, *17*, 2596.
(21) Li, D.; Haneda, H.; Labhsetwar, N. K.; Hishita, S.; Ohashi, N. *Chem. Phys. Lett.* **2005**, *401*, 579.
(22) Zhou, J. K.; Lv, L.; Yu, J.; Li, H. L.; Guo, P.-Z.; Sun, H.; Zhao, X. S. *J. Phys. Chem. C* **2008**, *112*, 5316.
(23) Huang, D.; Liao, S.; Liu, J.; Dang, Z.; Petrik, L. *J. Photochem. Photobiol. A* **2006**, *184*, 282.
(24) Huang, D.; Liao, S.; Quan, S.; Liu, L.; He, Z.; Wan, J.; Zhou, W. *J. Mater. Sci.* **2007**, *42*, 8193.
(25) Tang, J.; Quan, H.; Ye, J. *Chem. Mater.* **2007**, *19*, 116.
(26) Luo, H.; Takata, T.; Lee, Y.; Zhao, J.; Domen, K.; Yan, Y. *Chem. Mater.* **2004**, *16*, 846.
(27) Hong, X.; Wang, Z.; Cai, W.; Lu, F.; Zhang, J.; Yang, Y.; Ma, N.; Liu, Y. *Chem. Mater.* **2005**, *17*, 1548.
(28) Liu, G.; Chen, Z.; Dong, C.; Zhao, Y.; Li, F.; Lu, G.; Cheng, H. *J. Phys. Chem. B* **2006**, *110*, 20823.
(29) Long, M.; Cai, W.; Wang, Z.; Liu, G. *Chem. Phys. Lett.* **2006**, *420*, 71.
(30) Su, W.; Zhang, Y.; Li, Z.; Wu, L.; Wang, X.; Li, J.; Fu, X. *Langmuir* **2008**, *24*, 3422.
(31) Shannon, R. D. *Acta Crystallogr. A* **1976**, *32*, 751.
(32) http://www.webelements.com.
(33) Czoska, A. M.; Livraghi, S.; Chiesa, M.; Giamello, E.; Agnoli, S.; Granozzi, G.; Finazzi, E.; Valentin, C. D.; Pacchioni, G. *J. Phys. Chem. C* **2008**, *112*, 8951.
(34) Lin, H.; Kumon, S.; Kozuka, H.; Yoko, T. *Thin Solid Films* **1998**, *315*, 266.

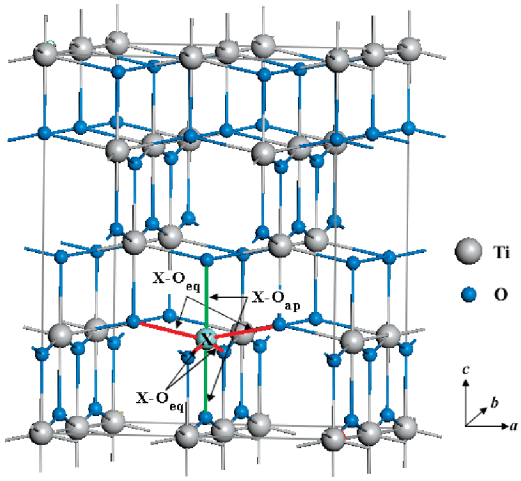

Figure 2. Forty-eight-atom 2 × 2 × 1 supercell model used to simulate X-doped anatase TiO_2 with X@Ti (X = F, Cl, Br, I). The XO_6 local geometry is described in terms of the two structural parameters $X-O_{eq}$ and $X-O_{ap}$.

package.[35,36] Our calculations employed a generalized gradient approximation, the Perdew−Wang 91 exchange-correlation functional;[37] the ultrasoft pseudopotential;[38] a cutoff energy of 400 eV for the plane-wave basis set; and a 4 × 4 × 4 *k*-mesh.[39] The convergence threshold for self-consistent iteration was set at 10^{-6} eV, and the lattice parameters and all the atomic positions were fully optimized until all components of the residual forces were smaller than 0.025 eV/Å. The density of states (DOS) for each optimized X-doped TiO_2 structure was calculated by using the tetrahedron method with Blöchl corrections.

3. Defect Formation Energies

To determine the energy required for substituting X for either O or Ti in TiO_2, we calculate the defect formation energy, E_f^X, which is defined as

$$E_f^X = E_{X-doped} - E_{undoped} - \mu_X + \mu_R \quad (1)$$

where $E_{X-doped}$ is the total energy for the 2 × 2 × 1 supercell of X-doped TiO_2, $E_{undoped}$ the total energy for the 2 × 2 × 1 supercell of undoped TiO_2, μ_X the chemical potential of X, and μ_R the chemical potential of the atom replaced by X (i.e., O or Ti). The chemical potentials of Ti and O, which depend on whether TiO_2 is grown under O-rich or T-rich growth conditions,[40] were taken from our previous calculations,[41] while the chemical potential μ_X was obtained from the energy calculated for X_2 (=F_2, Cl_2, Br_2, I_2). The E_f^X values, calculated with and without geometry optimization, are summarized in Table 1.

It is noted from eq 1 that the substitutional doping is energetically more favorable as the E_f^X value becomes smaller. From the E_f^X values of Table 1, the following trends are observed:

(a) For each X-doped TiO_2, the optimized structure has a lower defect formation energy than does the unoptimized structure, as expected. (Details of the structural changes associated with doping are discussed in section 4.)

Table 1. Defect Formation Energies E_f^X (in eV) Calculated for the Optimized and Unoptimized Structures of X-Doped Anatase TiO_2 with X@O and X@Ti (X = F, Cl, Br, and I)

	X	O-rich	Ti-rich
X@O	F	−1.01 (0.51)[a]	−5.65 (−4.13)[a]
	Cl	3.03 (9.04)	−1.61 (4.39)
	Br	4.66 (13.70)	0.02 (9.06)
	I	8.38 (22.89)	3.74 (18.25)
X@Ti	F	6.72 (7.95)	16.01 (17.23)
	Cl	3.77 (5.28)	13.05 (14.57)
	Br	2.20(4.04)	11.48 (13.32)
	I	0.65 (2.77)	9.93(12.05)

[a] The numbers for the optimized and unoptimized structures are given outside and inside the parentheses, respectively.

(b) For X-doped TiO_2 with X@O, the doping is energetically much more favorable under the Ti-rich than under the O-rich growth condition, and becomes more difficult in the order F < Cl < Br < I. The latter indicates that it is more difficult to substitute a larger and less electronegative X for an O atom. The formation of F-doped TiO_2 is thermodynamically favorable (i.e., $E_f^X < 0$) under both Ti-rich and O-rich conditions and so is that of Cl-doped under Ti-rich condition.

(c) For X-doped TiO_2 with X@Ti, the doping is energetically much more favorable under the O-rich than under the Ti-rich growth condition, and becomes more difficult in the order I < Br < Cl < F. The latter indicates that it is more difficult to substitute a smaller and more electronegative X for a Ti atom.

(d) Under O-rich growth condition, it is energetically more favorable to substitute Br and I for a Ti site than for an O site, while it is energetically more favorable to substitute F and Cl for an O site than for a Ti site.

(e) Under Ti-rich growth condition, it is energetically more favorable to substitute all X (=F, Cl, Br, I) for an O site than for a Ti site.

In the previous studies of N-, S-, and P-doped TiO_2 [41,42] as well as C-doped TiO_2,[43] it was found that replacing an O atom is more favorable under Ti-rich growth condition, as is replacing a Ti atom under O-rich growth condition. In general, therefore, in doping TiO_2 with a main group element, replacing an O atom is more favorable under Ti-rich condition, and replacing a Ti atom is more favorable under O-rich condition.

4. Effects of Halogen-Doping on Structure

The effect of an X-dopant on the structure of X-doped TiO_2 can be seen from the unit cell parameters and the local geometry around X. Table 2 summarizes the cell parameters and the local XTi_3 geometry (see Figure 1) for X-doped TiO_2 with X@O, and Table 3 summarizes the cell parameters and the local XO_6 geometry (see Figure 2) for X-doped TiO_2 with X@Ti. The crystal structure of undoped anatase TiO_2 is tetragonal. The crystal structure of X-doped TiO_2 with

(35) Kresse, G.; Furthmuller, J. *Comput. Mater. Sci.* **1996**, *6*, 15.
(36) Kresse, G.; Furthmuller, J. *Phys. Rev. B* **1996**, *54*, 11169.
(37) Perdew, J. P.; Chevary, J. A.; Vosko, S. H.; Jackson, K. A.; Pederson, M. R.; Singh, D. J.; Fiolhais, C. *Phys. Rev. B* **1992**, *46*, 6671.
(38) Vanderbilt, D. *Phys. Rev. B* **1990**, *41*, 7892.
(39) Monkhorst, H. J.; Pack, J. D. *Phys. Rev. B* **1976**, *13*, 5188.
(40) Walle, C. G. V. d.; Neugebauer, J. *J. Appl. Phys.* **2004**, *95*, 3851.
(41) Yang, K.; Dai, Y.; Huang, B. *J. Phys. Chem. C* **2007**, *111*, 12086.
(42) Yang, K.; Dai, Y.; Huang, B. *J. Phys. Chem. C* **2007**, *111*, 18985.
(43) DiValentin, C.; Pacchioni, G.; Selloni, A. *Chem. Mater.* **2005**, *17*, 6656.

Table 2. Optimized Structural Parameters of X-Doped Anatase TiO_2 (X = F, Cl, Br, I) with X@O

	undoped	X = F	X = Cl	X = Br	X = I
a, Å	3.776	3.817	3.884	3.928	3.947
b, Å	3.776	3.817	3.810	3.805	3.802
c, Å	9.486	9.540	9.519	9.533	9.607
$X-Ti_{eq}$, Å	1.930	2.034	2.208	2.289	2.392
$X-Ti_{ap}$, Å	1.973	2.224	2.507	2.611	2.663
θ, deg	156.2	161.0	175.3	179.0	175.8

Table 3. Optimized Structural Parameters of X-Doped Anatase TiO_2 (X = F, Cl, Br, I) with X@Ti

	undoped	X = F	X = Cl	X = Br	X = I
a, Å	3.776	3.798	3.804	3.810	3.834
b, Å	3.776	3.798	3.803	3.811	3.835
c, Å	9.486	9.673	9.647	9.675	9.658
$X-O_{eq}$, Å	1.930	1.984	1.907	1.946	2.004
$X-O_{ap}$, Å	1.973	2.436	2.272	2.284	2.067

X@Ti remains essentially tetragonal (Table 3) for all X = F, Cl, Br, and I, because the XO_6 octahedron has a local S_4 symmetry (Figure 2). In contrast, the crystal structure of X-doped TiO_2 with X@O becomes orthorhombic for X = Cl, Br, and I with the *a*-axis length becoming greater than the *b*-axis length (Table 2). The reason for this change is that the "T-shaped" XTi_3 has a local C_{2v} symmetry with the $X-Ti_{ap}$ bond as the rotational axis and the two $X-Ti_{eq}$ bonds approximately along the *a*-direction (Figure 1). Therefore, as X becomes larger, the *a*-axis length increases faster than does the *b*-axis length.

For X-doped TiO_2 with X@O, Table 2 shows that the lattice parameters *a*, *b*, and *c* increase gradually in the order *F* < Cl < Br < I, and so do the equatorial and the axial X−Ti bond lengths, $X-Ti_{eq}$ and $X-Ti_{ap}$, respectively (Figure 1). The ∠Ti−X−Ti angle θ between the two $X-Ti_{eq}$ bonds is larger than the corresponding ∠Ti−O−Ti angle of undoped TiO_2. This is expected, because more room around X is needed as the X^- ion becomes larger and because the size of X^- ion increases in the order F < Cl < Br < I. It should be mentioned that the existence of X-Ti bonds in X-doped TiO_2 samples (X = F, Cl, Br, I) has been confirmed by X-ray photoelectron spectroscopy (XPS) measurements.[15,26,30,44]

For X-doped TiO_2 with X@Ti, Table 3 summarizes the cell parameters and the local XO_6 geometry (Figure 2). The cell parameters of X-doped TiO_2 are greater than those of undoped TiO_2 and increase gradually in the order F < Cl < Br < I. The IO_6 octahedron of I-doped TiO_2 is symmetrical in that the $I-O_{eq}$ bonds are nearly the same in length as the $I-O_{ap}$ bonds (2.004 vs 2.067 Å, respectively). Similarly, in S-doped TiO_2 with S@Ti, the SO_6 local structure is also quite symmetrical (i.e., $S-O_{eq}$ = 1.896 Å, $S-O_{ap}$ = 1.902 Å).[42] This is due in part to the fact that the electronegativities of S and I are nearly the same (i.e., 2.69 and 2.74, respectively).[32] In X-doped TiO_2 (X = F, Cl, Br), however, the $X-O_{eq}$ bond is considerably shorter than $X-O_{ap}$ (i.e., 1.984 vs 2.436 Å for X = F, 1.907 vs 2.272 Å for X = Cl, and 1.946 vs 2.284 Å for X = Br). As will be discussed in section 5.2, the nearly symmetrical XO_6 octahedron in I- and S-doped TiO_2 arises from the fact that the I and S atoms at a Ti site exist respectively as I^{5+} (s^2) and S^{4+} (s^2) ions with no Jahn−Teller instability. In contrast, the axially elongated XO_6 octahedron in X-doped TiO_2 (X = F, Cl, Br) is related to the fact that the F, Cl, and Br atoms at a Ti site exist respectively as F^{3+} (s^2p^2), Cl^{4+} (s^2p^1), and Br^{4+} (s^2p^1) ions with Jahn−Teller instability.

5. Band Gap and Band Gap States of Doped TiO_2

5.1. X-Doped TiO_2 with X@O. Our DFT calculations led to the band gap of about 2.10 eV at Γ point for undoped TiO_2, which is smaller than the experimental value 3.20 eV. This underestimation of the band gap is due mainly to the well-known shortcoming of exchange-correction functional in describing excited states. For F-, Cl-, Br-, and I-doped TiO_2, the band gaps are calculated to be about 2.06, 1.90, 1.80, and 1.40 eV, respectively. Since the experimental band gap of undoped TiO_2 is obtained by adding 1.10 eV to the calculated band gap, it is practical to correct the underestimation of the band gaps of halogen-doped TiO_2 by adding 1.10 eV to the calculated band gap (i.e., "scissors operation"). Thus, the corrected band gaps of F-, Cl-, Br-, and I-doped TiO_2 are 3.16, 3.00, 2.90, and 2.50 eV, respectively. Namely, the band gap of X-doped TiO_2 decreases in the order F > Cl > Br > I. It should be noted that the band gap of X-doped TiO_2 is not related to the energy gap between the Ti t_{2g}- and e_g-block bands but to how the energy separation between the O p-block and the Ti t_{2g}-block bands of undoped TiO_2 is modified by X-doping.

Then, the band gap of F-doped TiO_2 is very slightly smaller than that of undoped TiO_2 (by about 0.04 eV). Thus, it is understandable that experimentally one observes either a very slight decrease (about 0.05 eV [15]) or no change [19−21,23,24] in the band gap. In any event, F-doping is not a good choice for extending the optical absorption edge of TiO_2 into the visible region. For Cl- and Br-doped TiO_2, a pronounced band gap narrowing (about 0.2 and 0.3 eV, respectively) is observed, in good agreement with the experimentally observed reduction of the band gap by about 0.2−0.3 eV in Cl/Br-codoped TiO_2.[26] For I-doped TiO_2, a more significant band gap reduction (about 0.7 eV) is observed, so that a significant red-shift of absorption edge is expected. The experimental band gap of undoped TiO_2 is about 3.2 eV and hence absorbs no visible light, so pure TiO_2 exhibits white color. Cl- and Br-doped TiO_2 have band gaps of about 3.0 and 2.9 eV, respectively, corresponding to the optical absorption edges of about 413 and 428 nm, respectively, so they should exhibit a green-yellow color. For I-doped $TiO_2$with I@O, the calculated band gap is about 2.5 eV after the use of a scissors operator, showing that blue light will be absorbed, and hence, the I-doped TiO_2 should exhibit yellow color.

To examine the origin of the electronic structure modification of X-doped TiO_2, we calculated their DOS plots. The partial DOS plots presented in Figure 3 show that most F 2p states are located in the lower-energy range of the VB and do not contribute to the reduction of the optical band gap. In Cl- and Br-doped TiO_2, the states associated with

(44) Gao, C.; Song, H.; Hu, L.; Pan, G.; Qin, R.; Wang, F.; Dai, Q.; Fan, L.; Liu, L.; Liu, H. *J. Lumin.* **2008**, *128*, 559.

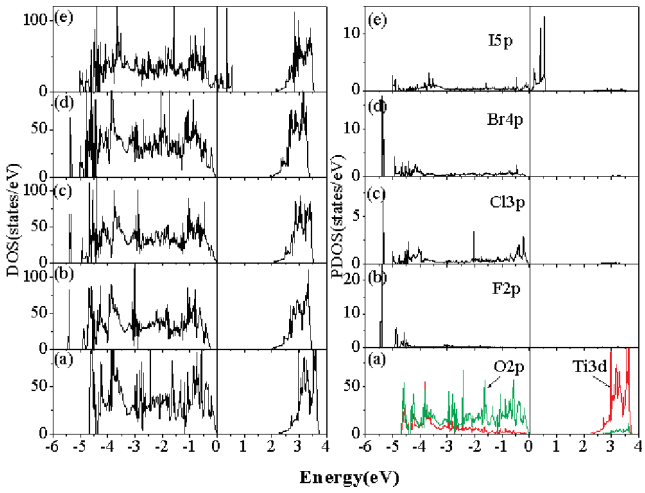

Figure 3. Total and partial DOS plots (left and right panels, respectively) calculated for undoped and X-doped anatase TiO_2 with X@O (X = F, Cl, Br, I): (a) undoped, (b) F-doped, (c) Cl-doped, (d) Br-doped, and (e) I-doped anatase TiO_2. The energy is measured with respect to the VBM of undoped anatase TiO_2.

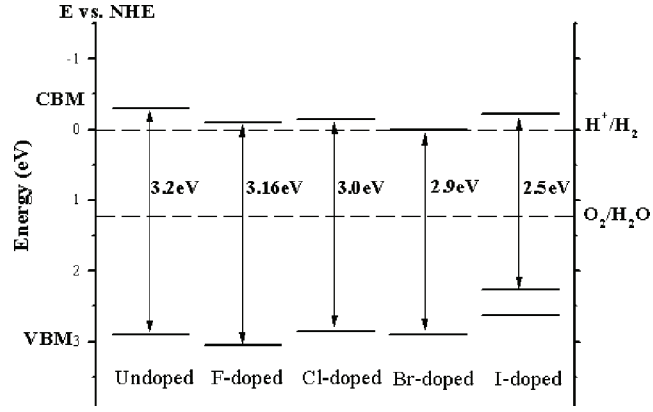

Figure 4. Comparison of the calculated VBM and CBM positions of X-doped anatase TiO_2 with X@O (X = F, Cl, Br, I) from the DFT calculations with the corresponding experimental values of undoped TiO_2. The VBM and CBM values are given with respect to the normal hydrogen electrode (NHE) potential.

the dopants are raised in energy relative to those in F-doped TiO_2. This increases the width of the VB and reduces the band gap with respect to that in the F-doped TiO_2 (by about 0.16 and 0.24 eV for Cl- and Br-doped TiO_2). For I-doped TiO_2, some I 5p states extend into the band gap from the VB edge of undoped TiO_2 by about 0.6 eV, which is largely responsible for the band gap reduction.

The ability of a semiconductor to transfer a photon-excited electron to the adsorbed species on its surface is governed by the positions of its CBM and VBM with respect to the redox potentials of the adsorbate,[45] and thus, the photocatalytic ability of TiO_2 is determined to a great extent by the positions of its CBM and VBM. Thermodynamically, the VBM of TiO_2 should lie below the redox level of the adsorbed species so that the photoinduced hole can capture an electron from the adsorbed species, while the CBM should lie above the redox level of the adsorbed species for the photoinduced electron to transfer to the adsorbed species. To study how halogen-doping influences the photocatalytic activity of TiO_2, we determine the CBM and VBM of undoped and X-doped TiO_2 systems. The resulting VBM and CBM values are presented in Figure 4, where the VBM and CBM of undoped TiO_2 (with respect to the normal hydrogen electrode potential) were taken from the experimental values.[43]For X-doped TiO_2, the CBMs were obtained from the DOS plots according to the relative positions with respect to that of undoped TiO_2, and then the VBMs were obtained from the corrected band gaps.

Figure 4 shows that the CBM and VBM of F-doped TiO_2 are lowered from those of undoped TiO_2 by 0.20 and 0.16 eV, respectively. The lowering of the VBM indicates that F-doped TiO_2 has a stronger oxidation power and is hence consistent with the observation that F-doped TiO_2 has a higher photocatalytic activity than does undoped TiO_2.[13−15,19,24,25] For Cl-doped TiO_2, the CBM is lowered by about 0.15 eV, while the VBM is raised by about 0.05 eV relative to the corresponding values of undoped TiO_2. Thus, Cl-doped TiO_2 should have a reduced ability for oxidation and reduction, which is consistent with the experimental observation that Cl-doped TiO_2 has lower water-splitting power than that of undoped TiO_2 under UV irradiation.[26] The VBM of Br-doped TiO_2 is the same as that of undoped TiO_2, so Br-doped TiO_2 and undoped TiO_2 should have the same oxidation power. The CBM of Br-doped TiO_2 is lowered from that of undoped TiO_2 by about 0.3 eV, so that Br-doped TiO_2 would have lower ability to reduce H^+ to H_2 than does undoped TiO_2. The CBM of I-doped TiO_2 is slightly lowered from that of undoped TiO_2. However, the VBM of I-doped TiO_2 is raised strongly from that of undoped TiO_2, so visible-light photocatalytic activity is expected for I-doped TiO_2.

5.2. X-Doped TiO_2 with X@Ti. Our discussion in section 3 showed that, under O-rich growth condition, it is energetically more favorable to substitute Br and I for a Ti site than for an O site. We now examine the electronic structures of X-doped TiO_2 with X@Ti (X = F, Cl, Br, I). The total and partial DOS plots calculated for these systems are presented in Figure 5.

Figure 5a shows that the VB and CB of I-doped anatase TiO_2 are essentially the same as those of undoped TiO_2. However, I-doping introduces a doubly occupied band gap state 0.6 eV above the VBM. The partial DOS plots show that this band gap state consists mostly of I 5s states and the 2p states of its neighboring O atoms, and that the I 5p states contribute to the CBs. This indicates that the dopant I atom at a Ti-site exists as an I^{5+} (s^2) cation, as found experimentally.[27,28] The presence of an I^{5+} (s^2) cation in the IO_6 octahedron means that there is no Jahn−Teller instability in the IO_6 octahedron, which explains why the IO_6 structure is nearly symmetrical. From the DOS plots for S-doped TiO_2 with S@Ti,[39] it is also found that the S atom exists as an S^{4+} (s^2) ion, so the SO_6 octahedron is nearly symmetrical.

The Fermi level of I-doped TiO_2 (Figure 5a) is pinned at 0.2 eV above the CBM so that iodine is effectively acting

(45) Linsebigler, A. L.; Lu, G.; Yates, J. T. *Chem. Rev* **1995**, *95*, 735.

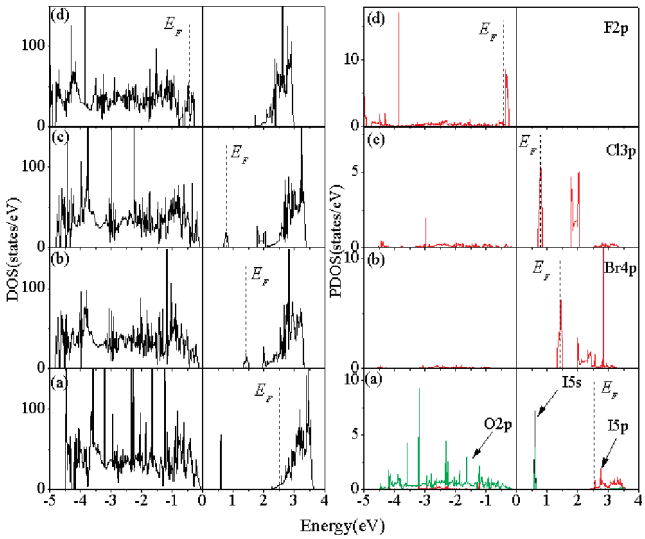

Figure 5. Total and partial DOS plots (left and right panels, respectively) calculated for X-doped anatase TiO_2 with X@Ti (X = F, Cl, Br, I): (a) I-doped, (b) Br-doped, (c) Cl-doped, and (d) F-doped. The energy is measured with respect to the VBM of undoped anatase TiO_2.

as an n-type dopant in TiO_2, as found for I-doped ZnTe.[46] As a consequence, the optical band gap of I-doped anatase TiO_2 is smaller than that of undoped TiO_2 by ~0.4 eV, which is consistent with the experimental red-shift of absorption edge in I-doped anatase TiO_2 (i.e., about 460 nm; see Figure 8 of ref 28). In essence, therefore, the optical band gap of I-doped TiO_2 is reduced from that of undoped TiO_2,[27,28] because the filled I 5s states lie above the valence band top. The band gap reduction provides a natural explanation for the increased photocatalytic efficiency of I-doped TiO_2 in the UV/vis region. I-doped $TiO_2$with I@Ti has an optical band gap of approximately 2.8 eV, corresponding to the blue light, and hence exhibits a yellow color.[27,28,30] The charge balance in I-doped TiO_2 with I@Ti (and hence with I^{5+} ions) suggests the presence of some Ti^{3+}cations, which are associated with the filled states around the CBM. Thus, it is possible that the color of I-doped $TiO_2$with I@Ti is also influenced by the Ti^{3+} to Ti^{4+} intervalence transition.

Figure 5 shows that the electronic structures of F-, Cl-, and Br-doped TiO_2 are strikingly different from that of I-doped TiO_2 in the nature of the band gap states. Unlike the case of I-doped TiO_2, the Cl 3s and Br 4s states of Cl- and Br-doped TiO_2, respectively, do not occur above the VBM. However, there occur singly filled Cl 3p and Br 4p states in between the VBM and CBM in Cl- and Br-doped TiO_2, respectively. This means that the Cl and Br atoms occupying a Ti site in anatase TiO_2 exist as Cl^{4+} (s^2p^1) and Br^{4+} (s^2p^1) ions, respectively, which gives rise to Jahn−Teller instability to the XO_6 octahedra (X = Cl, Br). Consequently, the XO_6 (X = Cl, Br) in Cl- and Br-doped TiO_2 has an axially elongated octahedral structure as discussed in section 4. For F-doped TiO_2, the F 2p states are lowered in energy such that the empty F 2p states corresponding to the empty Cl 3p of Cl-doped TiO_2 (and the empty Br 4p states of Br-doped TiO_2) lie just above the Fermi level. To a first approximation, therefore, the F atom exists as a F^{3+} (s^2p^2) ion so that the FO_6 octahedron shows an axially elongated octahedral structure due to the associated Jahn−Teller distortion. The fact that the F, Cl, Br, and I atoms exist as F^{3+}, Cl^{4+}, Br^{4+}, and I^{5+} ions at a Ti site is understandable given their electronegativities.

To probe the effect of different doping levels of halogen on the electronic structure, further calculations were carried out for X-doped TiO_2 by using a 96-atom (1.04 atom %) supercell. The electronic structures of X-doped TiO_2 (X = F, Cl, Br, I) at this doping level (96-atom supercell, i.e., 1.04 atom %) are nearly same as those found for the 48-atom supercell calculations (2.08 atom %). Thus, our results are valid for the low doping level in which interactions between dopant sites are negligible.

6. Concluding Remarks

In the present first-principles DFT study of halogen-doped anatase TiO_2, we considered the substitutional doping, namely, the halogen doping at oxygen and titanium sites. Our results lead to the following conclusions:

(a) For X-doped TiO_2 with X@O, the doping is energetically much more favorable under the Ti-rich than under the O-rich growth condition and becomes more difficult in the order F < Cl < Br < I. For X-doped TiO_2 with X@Ti, however, the doping is energetically much more favorable under the O-rich than under the Ti-rich growth condition and becomes more difficult in the order I < Br < Cl < F.

(b) Under O-rich growth condition, it is energetically more favorable to substitute Br and I for a Ti site than for an O site, while it is energetically more favorable to substitute F and Cl for an O site than for a Ti site. Under Ti-rich growth condition, it is energetically more favorable to substitute all X (=F, Cl, Br, I) for an O site than for a Ti site.

(c) For I-doped TiO_2 with I@Ti, the I atoms are present as I^{5+} (s^2) ions so that the IO_6 octahedron has no Jahn−Teller instability and hence has a nearly symmetrical structure. For X-doped TiO_2 with X@Ti (X = F, Cl, Br), however, the F, Cl, and Br atoms are present as F^{3+} (s^2p^2), Cl^{4+} (s^2p^1), and Br^{4+} (s^2p^1) ions, respectively, so the XO_6 octahedron has Jahn−Teller instability and hence has an axially elongated structure. I-doped TiO_2 with I@Ti has a doubly occupied band gap state made up of the I 5s orbitals, while X-doped TiO_2 with X@Ti (X = Cl, Br) has a singly occupied band gap state made up of the X *n*p orbitals (*n* = 3 and 4 for X = Cl and Br, respectively).

(d) The band gap state of I-doped TiO_2 with I@Ti lies 0.6 eV above the VBM and is primarily responsible for why the optical band gap of I-doped TiO_2 is reduced from that of undoped TiO_2 and why I-doped TiO_2 exhibits an increased photocatalytic efficiency of in the UV/vis region compared with undoped TiO_2.

(e) For X-doped TiO_2 with X@O (X = F, Cl, Br), the VBM and CBM values determined by the DFT calculations are consistent with experiments. I-doped TiO_2 with I@O is predicted to have a significant band gap reduction compared

(46) Kuhn, W.; Wagner, H. P.; Stanzl, H.; Wolf, K.; Worle, K.; Lankes, S.; Betz, J.; Worz, M.; Lichtenberger, D.; Leiderer, H.; Gebhardt, W.; Triboulet, R. *Semicond. Sci. Technol.* **1991**, *6*, A105.

with that of undoped TiO_2, because its band gap state made up of the I 5p orbitals lies about 0.6 eV above the VBM.

Acknowledgment. This work is supported by the National Basic Research Program of China (973 program, Grant No. 2007CB613302), National Natural Science Foundation of China under Grant No. 10774091, Natural Science Foundation of Shandong Province under Grant No. Y2007A18, and the Specialized Research Fund for the Doctoral Program of Higher Education 20060422023. M.-H.W. is thankful for the support of the Office of Basic Energy Sciences, Division of Materials Sciences, U.S. Department of Energy, under Grant DE-FG02-86ER45259.

CM801741M